

Sorption of Aldrich Humic Acids onto Hematite: Insights into Fractionation Phenomena by Electrospray Ionization with Quadrupole Time-of-Flight Mass Spectrometry

*PASCAL REILLER**, *BADIA AMEKRAZ** and *CHRISTOPHE MOULIN*

CEA, CE Saclay, Nuclear Energy Division, DANS/DPC/SECR, Laboratoire de Spéciation des Radionucléides et des Molécules, Bâtiment 391, BP 11, F-91191 Gif sur Yvette Cedex, France.

pascal.reiller@cea.fr, +33 1 6908 4312 ;badia.amekraz@cea.fr, +33 1 6908 8034; Fax +33 1 6908 5411

Abstract.

Sorption induced fractionation of purified Aldrich humic acid (PAHA) on hematite is studied through the modification of electrospray ionization (ESI) quadrupole time-of-flight (QToF) mass spectra of supernatants from retention experiments. The ESI mass spectra show an increase of the “mean molecular masses” of the molecules that constitutes humic aggregates. The low molecular weight fraction (LMWF; $m/z \leq 600$ Da) is preferentially sorbed compared to two other fractions. The resolution provided by ESI-QToF mass spectrometer in the low-mass range provided evidence of further fractionation induced by sorption within the LMWF. Among the two latter fractions, the high

molecular weight fraction (HMWF; $m/z \approx 1700$ Da) seems to be more prone to sorption compared to the intermediate molecular weight fraction (IMWF; $m/z \approx 900$ Da). The IMWF seems to be more hydrophilic as it should be richer in O, N and alkyl C from the proportion of even mass, and poorer in aromatic structures from mass defect analysis in ESI mass spectra.

Keywords: Humic Substances, Fractionation, Retention, Iron Oxides, ESI-MS

Introduction

Humic substances (HS) are found in every type of aquatic and terrestrial environments and strongly influence the environmental chemistry of metallic cations in general and of radionuclides in particular. The chemistry and migration properties of metallic cations can be largely controlled by their interactions with HS (1, 2). Recent developments seem to indicate that humic acids (HA) are heterogeneous mixtures of molecules self-assembled in supramolecular colloidal aggregates by multiple noncovalent interactions (3-8). HA can be sorbed on almost every type of mineral surfaces. The general affinity of HA toward mineral surfaces not only induces modifications of physicochemical properties (9, 10), but also provokes structural modifications, in particular the fractionation of aggregates (10-14). Variations of apparent molecular weights (MW) of HA were noted, the extent of which depends on their origin and the nature of the mineral phases. Preferential sorption of higher MW fractions were evidenced for lacustrine and aquatic NOM on metallic oxides and clays (10, 12), whereas a preferential sorption of lower MW fractions on iron oxides using Aldrich HA was evidenced (13, 14). Fractionation phenomena also depend on the nature of mineral phases (13), and are kinetically controlled (9, 15). The majority of the work on NOM sorption has been focused predominantly on HS from aquatic sources, and as a result, there is not as much of information on the fractionation of terrestrial HS (13, 16). Particularly, the influence of the mineralogy was recently reported (17, 18).

A difference between the fractionation behavior of terrestrial and aquatic HS makes such studies even more important in the field of nuclear waste disposal assessment. The outcome of the

fractionation phenomena of HS is of importance in the field of modeling the interaction in ternary systems consisting of metallic cations, HS and a mineral surface. Indeed, the behavior of metallic cations in these systems has been proved to be difficult to model as additivity of interaction models is often not respected (19, 20), and addition order plays an important role on the final result (21-23).

Over the past two decades, detailed investigations on sorption induced changes of HS properties have been hampered by their heterogeneity, and it is still difficult to assess the detailed structural features that control fractionation processes. The advent of the electro-spray ionization (ESI) technique, which generates gas-phase ions directly from molecules in solution, has demonstrated a unique potential toward HS structural analysis (24-28). Some works have attempted to take advantage of the mass resolving power, and tandem mass analysis (MS/MS) offered by a hybrid quadrupole time-of-flight (Q-ToF) instrument (5-7, 29). Possible parameters that complicate interpretation of ESI-MS mass spectra of HS include formation of multiple-charged ions, charged aggregates, sample fragmentation, and variations in ionization efficiencies among compounds within mixtures. While there is ongoing debate over whether some molecules may form multiple-charged species and/or charged aggregates, a consensus is emerging that HS occurs primarily as individual singly-charged species, and it becomes apparent that generally peaks representing doubly charged species are minor and do not greatly affect the molecular weight distribution of humic substances (30-32). The extent of HS fragmentation during the desorption-ionization process is an important concern but is difficult to determine. No direct evidence was found for fragmentation of humic and fulvic acid in the ESI source (31). The main limitation of ESI-MS in the study of HS was due to variations in ionization efficiencies among compounds within the mixtures. The differences in ionization efficiencies affect the relative abundances of compounds within the spectrum and limit the ability of the technique to obtain quantitative information. As an example, the determination of mean molecular mass of HS from mass distributions is more reliable when samples were fractionated by size exclusion chromatography (SEC) to reduce the polydispersity before ESI-MS analysis (7, 32). Nevertheless, despite the lack of

knowledge about response factors for individual humic molecules, it is now well-demonstrated that mass distributions in ESI mass spectra carry valuable information for the characterization of mixtures. Recently, the use of ESI-MS has allowed the observation of organic mixtures modifications in natural systems (33-35). Hence, with the use of ESI-MS, one should address the question of the fractionation of HS during sorption experiments. The purpose of this study is to have a closer insight on the effect of sorption on the fractionation of purified Aldrich humic acid (PAHA) after sorption experiment on hematite. Even if the origin of this humic extract is rather obscure, and knowing that it cannot represent the heterogeneity of all “real” samples, it has often been shown that its compartment was in line with other natural environmental samples (13, 23, 36-38). Fractionation trends were investigated at steady-state (24 h reaction) and $\text{pH} \approx 7$, and varying initial PAHA concentration conditions with estimation of MW values and composition changes by ESI-MS. This pH value seems to be a good compromise between efficient sorption and optimal signal. Moreover, PAHA and colloidal hematite were chosen as model systems due to the available data in the literature for the sake of comparison.

Experimental Section

Materials. PAHA has been used in a protonated form. Its main characteristics are detailed elsewhere (37). The H/C and O/C ratios are respectively of 0.97 and 0.51, close to values determined otherwise, i.e. 0.98-0.95 and 0.52-0.50 (39, 40). This could lead to the classification of a terrestrial HS (41), even if the ^{13}C NMR spectrum is close to humics from brown coal (39, 40). The colloidal hematite suspension was obtained from AEA Harwell. Its characterization and HS sorption properties are detailed elsewhere (38, 42, 43).

Preparation of suspensions for sorption experiments. The sorption experiments were conducted according to a batch procedure at room temperature in polycarbonate vials sealed with screwcaps (Ultraplus Centrifugeware, 3430-1610, Nalgene). The rinsing protocol has been detailed elsewhere (23, 38). The concentration of hematite suspensions were fixed at the desired concentration by diluting the rinsed solution in Milli-Q water and by adding aliquots of PAHA stock solution. No attempt was made

to fix ionic strength in the solutions since it was observed to considerably alter the ESI-MS response. The pH values of the suspensions were adjusted using HClO₄, to minimize absorbance interference, or freshly prepared NaOH. The pH values were measured with a TACUSSEL pHmeter (PHM 220 MeterLab) equipped with a combined TACUSSEL electrode (Radiometer type XC 161). The electrode was standardized using commercial buffers (Prolabo, 4, 7). The obtained suspensions were shaken for 24 h to allow equilibration. The hematite colloids were separated from the liquid phase by ultracentrifugation (90 min; 50 000 rpm), and the pHs of the supernatants were measured. PAHA UV-visible spectra were acquired using a Cary 500 spectrophotometer using 1 cm quartz cells with MilliQ water as a reference, scanned from 350 to 200 nm at 100 nm/min. The quality of the absorbance data was verified by checking the linearity of the concentration dependence between 0 and 3.5 optical densities at 254 nm ($10 \leq [\text{PAHA}]^\circ \text{ (mg/L)} \leq 80$). The UV-visible spectrum of ultracentrifuged PAHA at pH 7 did not evidence any modification in the shape and only minor difference in intensity (5%, data not shown), suggesting only minor modification of the composition is induced through ultracentrifugation when hematite colloids are separated from PAHA.

ESI-MS Instrumentation and Analysis. The ESI mass spectrometer has already been described elsewhere (5, 6). The samples were introduced into the source with a syringe pump (Harvard Apparatus Cambridge, MA) with a flow rate set to 10 $\mu\text{L}/\text{min}$. [Glu]-fibrinopeptide B was used for mass calibration check, and optimal parameter tuning was performed using fulvic acids from Mol (Belgium) as in the previous studies. All ToF measurements were performed at a peak resolving power of about 4000 full width at half-maximum (fwhm) at m/z 500 which was the best compromise between resolution and the sensitivity required under our conditions, i.e. low [PAHA] after sorption experiments. Other settings optimized for sensitivity were ESI capillary voltage ($\pm 3500\text{V}$) and cone voltage (55V). Nitrogen was employed as both the drying and nebulization gas. The temperature of the source was held at 100°C. For MS analysis, Q1 was operated in RF-only mode with all ions transmitted into the pusher region of the ToF analyzer. Spectra were recorded by averaging 40 scans from m/z 100

to 3500 at a scan rate of 6s/scan. Processing was achieved by minimal baseline subtraction and smoothing of the raw data.

Number-averaged (\bar{I}_n) and weight-averaged (\bar{I}_w) mean molecular intensities were calculated by weighted summation of averaged and background subtracted ESI-MS spectra, assuming the following: (i) single charged ions, over the entire scan range as supported by previous studies (5, 6, 30-32), and (ii) a common ionization yield all over the populations. This latter approximation is rough and thus calculations provide information about changes in the composition of mixtures rather than mean molecular mass values (44). Under these approximations, the mean molecular intensity in number \bar{I}_n and in weight \bar{I}_w can be calculated using classical definitions.

Results and Discussions

To have a first sight at the fractionation phenomenon, UV-visible spectra of the initial PAHA solution (11 mg/L) and of supernatants at $\text{pH} \approx 7$ and initial PAHA concentration between 3.3 and 55 mg/L were acquired (see Supporting Information Table S1). These spectra were obtained after subtraction of the spectrum from a blank experiment with 500 mg/L hematite and no PAHA added at $\text{pH} = 7.13$. No quantification of sorption by UV-visible was performed as it is known to be biased (45).

It has been calculated that the theoretical saturation of all hematite sites by the PAHA sites required 3.5 mg of PAHA/L (38). Beyond this concentration, any excess of PAHA would thus be supposed not to interact with the surface.

The ratio of absorbance at 253 and 203 nm (see Figure S1 and S2 of the Supporting Information) indicates a variation in the proportion of polar groups linked to aromatic moieties (46). The A_{253}/A_{203} ratio remains at a maximum value of ca. 0.7 until 10 mg of PAHA/L, corresponding to the initial PAHA, i.e. $A_{253}/A_{203} = 0.67$, and then decreases with PAHA concentration enhancing the fact that aromatic chromophores with polar groups are fixed to the hematite surface. In absorbance the fractionation is thus only evidenced for low surface coverage.

The negative mode ESI-QToF mass spectra of initial PAHA and of supernatant were compared including the weak influence of initial PAHA concentration (Figure 1, and Figures S3 and S4 of the Supporting Information). This ionization mode provides distributions of abundant $(M-H)^-$ peaks due to the formation of singly charged species containing mostly anionic functionalities. The mass spectrum of the initial PAHA solution (Figure 1a) showed a distribution of peaks occurring at every m/z value between 100 and 2800 Dalton and shows trends similar to those observed in previous HS mass spectra (5, 6, 30, 44). A bimodal mass consisting in a first low molecular weight fraction (LMWF) centered around 400 m/z and an upper one, with much lower abundance, centered at about 1600 m/z . The mass distribution is much broader than previously reported for aquatic fulvic acids (200-600 Dalton) under identical experimental conditions, clearly indicating the highly heterogeneous nature of this HS sample. Intense peaks are also observed in the low-mass region (< 600 Da), probably showing degradation products derived from the biomass such as lipids, sterols and also free aliphatic acids (30).

Calculated values for \bar{I}_n and \bar{I}_w were 873 and 1228 Da respectively, in agreement with a previous finding in direct infusion (32). It must be noted that these determinations would only give an indication on \bar{M} of molecules that constitute colloidal aggregates and not on the equivalent size of colloidal aggregates obtained in high-performance size-exclusion chromatography (HPSEC). Thus, the \bar{I}_w value of PAHA calculated from the ESI mass spectrum is much lower than the apparent weight averaged \bar{M}_w value ($\bar{M}_w = 4890 \pm 47$ Da) obtained for the same material in HPSEC (13).

The ESI(-) spectra of supernatants with $[PAHA]^o$ (mg/L) comprised between 111 and 3.3 (Table S1 of the Supporting Information) were acquired (Figure 1b-d and Figure S4 of the Supporting Information). Mass spectra shapes are different from the bimodal distribution obtained before sorption. Thus, in the lower mass region, the relative signal intensities of sharp peaks increase. Conversely, the LMWF of PAHA decreased and is gradually replaced by two upper mass distributions with increasing sorption: an intermediate molecular weight fraction (IMWF) and a high molecular weight fraction

(HMWF) centered around 900 m/z and 1700 m/z respectively. Increasing signal intensities in the HMWF range of HS spectra were also observed using the SEC/ESI-MS approach which provides separation of the HS mixture in size-fractions to reduce polydispersity (47). The broadening of the mass distribution toward higher m/z values is likely due to the strong adsorption of the LMWF (< 600 Da) onto the mineral phase. This effect gives rise to a broadening of the mass distribution (100-3000 Da). As sorption increases ($[PAHA]^{\circ} < 30$ mg/L), the LMWF decreased and relative intensities of IMWF and HMWF varied: the proportion of the fraction $m/z > 1200$ Da is also lowered. This second effect leads to the detection of a consistent IMWF and a HMWF of low abundance in the ESI(-) spectra of the supernatant with $[PAHA]^{\circ} = 3$ mg/L (Figure 1d).

These results suggest that the LMWF is more likely fixed than the other ones to the surface at high initial PAHA concentration for a 24 h contact time. This can be compared with a previous observation and modeling (11, 15) on a comparable hematite sample, where the lowest molecular weight fraction of NOM (≤ 3 kDa in size) was preferentially fixed. Moreover, it was proposed that this fraction can be over represented at the surface for short contact time and high concentration of NOM (15). Moreover, through SEC-UV analysis it has been reported that the PAHA fraction with MW < 5000 Da in size was adsorbed more strongly onto hematite (13). As noted earlier, MW ranges determined by ESI-MS are smaller than the one based on SEC-UV, and likely provide deeper insight about the mass of individual HS molecules that are not adsorbed onto hematite.

Decreasing $[PAHA]^{\circ}$ leads to a more “balanced” situation where LMWF is still the major one sorbed but where the HMWF can also be bounded to hematite surface leaving some of IMWF compounds in solution.

These combined effects lead the \bar{I}_n and \bar{I}_w of PAHA fractions remaining in solution, calculated within the range of 100-2535 Da, to continuously increase with increasing sorption (Figure S5 of the Supporting Information).

The evolution of A_{253}/A_{203} indicated that PAHA components preferentially adsorbed onto the mineral surface were enriched in aromatic structures that contained polar groups. ESI-MS and UV-visible results appear to be consistent with the report that the smaller sized fractions of PAHA are the ones that have higher aromatic content and more acidic functional groups (48, 49) and contradict the saturation hypothesis. This is consistent with the conformation of the NOM aggregate structure sorbed (50). It is also demonstrated that those characteristics induce preferential adsorption to hematite, a fractionation pattern consistent with surface complexation via ligand exchange of small molecules.

These changes in MW values clearly indicate that a more efficient ionization of the IMWF and HMWF occurs in an ESI source when the dominance of LMWF is reduced due to its sorption. Then, one possible explanation may lie in chemical structures of the HS molecules. In ESI-MS, the suppression of analyte ion signal intensity caused by a higher concentration of hydrophobic species in solution is the result of ion partitioning between the surface volume and the bulklike core of the droplets (51, and references therein). It has been demonstrated that hydrophobic species compete against hydrophilic species for surface volume occupancy into which the gas-phase transfer is more favorable, and this likely accounts for their higher relative sensitivity in ESI experiments. This phenomenon has been pointed out recently in the case of terrestrial humic substances analysis (32).

Figure 2 shows an expanded mass region of the LMWF of initial PAHA from Figure 1. The PAHA mass spectrum (Figure 2a) is complex. Odd anion masses $(M-H)^-$ correspond to even molecular weights and to compounds with an even number of nitrogen atoms. Due to the low nitrogen content of PAHA, i.e. less than 1% in PAHA (37, 39, 40), it is generally assumed that odd m/z compounds contain primarily C, H, and O. The even m/z peaks are probably a mixture of peaks corresponding to the ^{13}C isotope of peaks at odd m/z , and peaks from compounds that may contain a nitrogen atom. Furthermore, peaks detected at every m/z are a mixture of various structures with the same nominal mass but slightly different exact masses that may further be resolved with ultrahigh resolution provided by FT-ICR mass spectrometry.

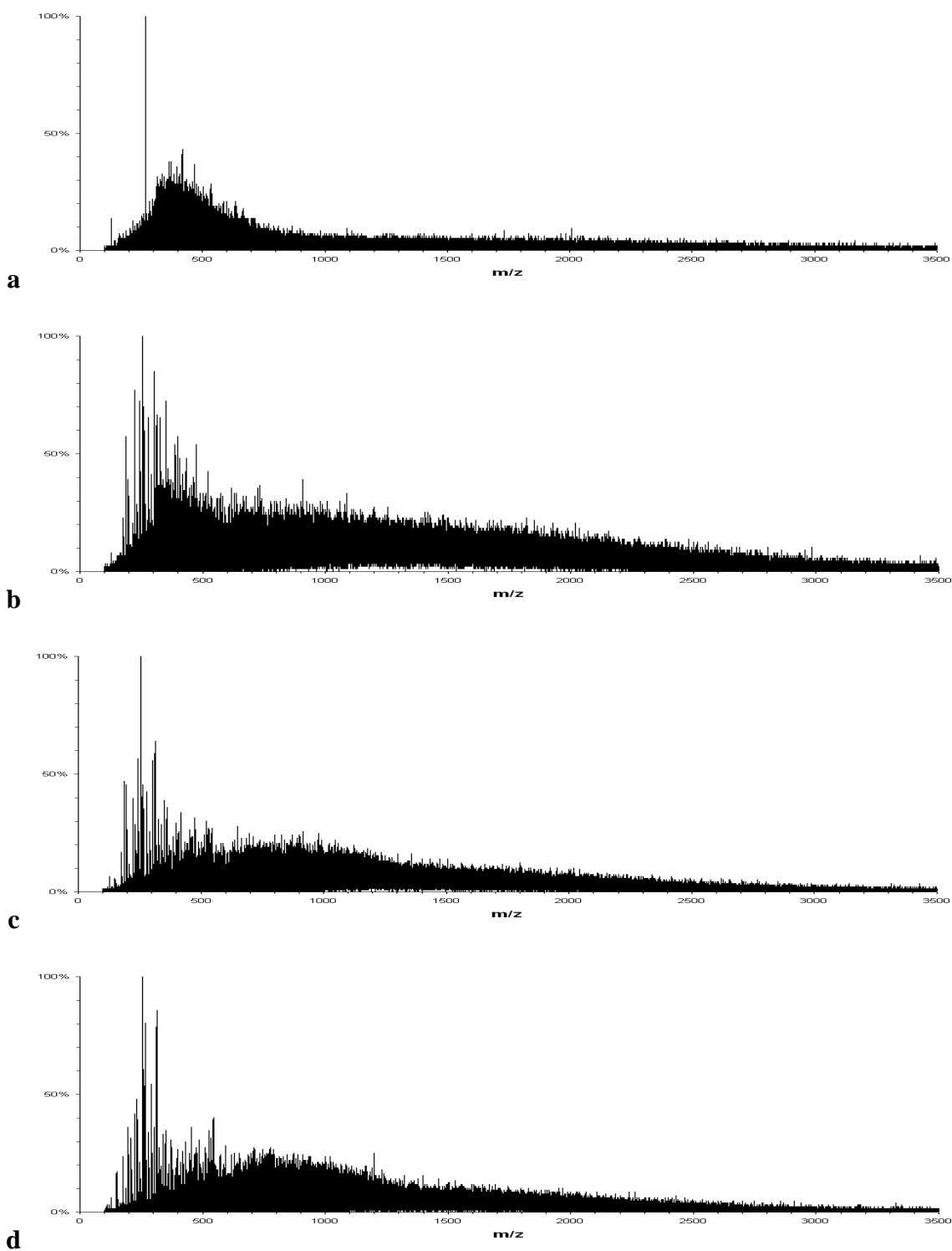


Figure 1: ESI Q-ToF negative ion mass spectra of PAHA (a) before sorption: 11 mg/L at $\text{pH} \approx 7$ (see Table S1; (b-d) after sorption at $\text{pH} \approx 7$, $[\alpha\text{-Fe}_2\text{O}_3] = 500$ mg/L, under varying initial [PAHA] : (b) 33 mg/L, (c) 11 mg/L, (d) 3.3 mg/L.

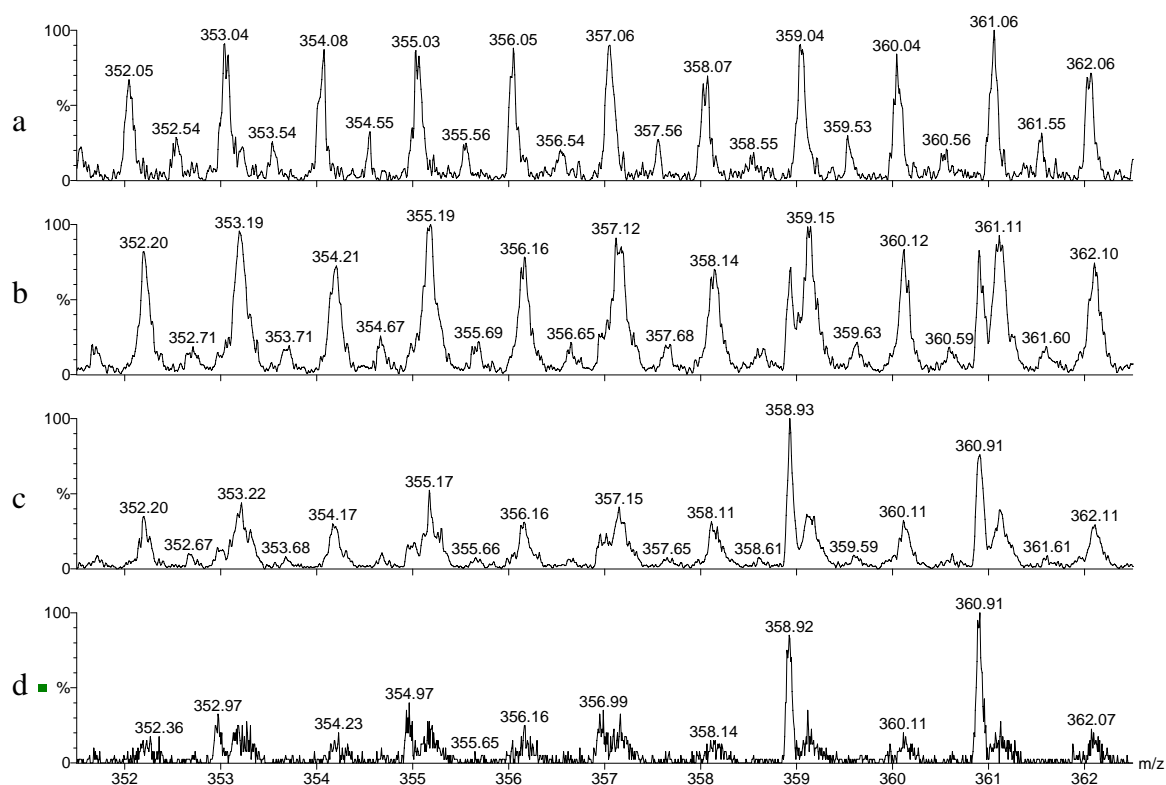


Figure 2: Detail in the range 444-466 Da of ESI Q-ToF negative ion mass spectra of PAHA (a) before sorption: 11 mg/L at $\text{pH} \approx 7$; (b-d) after sorption at $\text{pH} \approx 7$, $[\alpha\text{-Fe}_2\text{O}_3] = 500 \text{ mg/L}$, under varying initial [PAHA] : (b) 33 mg/L, (c) 11 mg/L and (d) 3.3 mg/L.

Deviation from nominal mass results from all possible elemental formulas that account for one nominal mass leading to a slightly different exact mass depending upon the number of constituent elements (C, H, N and O). Thus a high mass defect can be attributed to hydrogen-rich molecules, such as compounds with long alkyl substituents. Small mass defect can be attributed hydrogen poor molecules, such as substituted aromatic compounds with oxygen-containing functional groups. Moreover, negative mass defects occur when highly condensed aromatic structures are substituted with O, which has *per se* a negative mass defect (black carbon-like molecules) (52).

Interestingly, peaks detected in the low mass region ($< 500 \text{ Da}$) in the spectra of initial PAHA showed a low mass defect ($< 0.1 \text{ amu}$ for molecular weights of about 400 Da). This may indicate that the main structures in the hydrophobic LMWF are small aromatic structures (*e.g.*, polyphenolic

structures and lignin derived aromatic) with oxygen-containing functional groups (*e.g.*, hydroxyl-, carbonyl-, ester-, and carboxyl-substituted aromatics). The presence of mixtures of compounds is more evident in the mass spectra of the supernatants (Figure 2b-d). Mass spectra of supernatants are different than the initial PAHA sample. Sorption of LMWF onto the mineral phase causes regular change of the m/z pattern in the LMWF range clearly indicating fractionation trend among these components: peaks at each nominal mass are broader and are shifted towards higher mass defect (about 0.1 to 0.2 amu) suggesting sources of compounds that are not detected in initial PAHA ESI mass spectra. Furthermore, many of the peaks show a fraction occurring with a weak negative mass defect shift. The mass shift to higher mass defects likely indicates the presence of aromatic structures containing long-alkyl substituents, while the fraction occurring at lower mass defect suggests the presence of compounds with more condensed aromatic structures. These changes may likely indicate gradual sorption within the more hydrophobic molecules within the LMWF. Combinations of different adsorption active functional groups (such as carboxyl and hydroxyl) and aliphatic moieties clearly result in a range of sorption behaviors (53). These observations also demonstrate that differences in ionization efficiencies of the LMW compounds could cause the more polar ones to be more represented in the mass spectrum of the initial sample.

Figure 3 shows expanded mass regions of the IMWF of the Figure 2b, i.e. [PAHA]^o = 33 mg/L, after sorption onto 500 mg/L hematite. The pattern of this IMWF is quite complex compared to the LMWF and a striking feature is the lack of regularity observed otherwise in the peak distributions (5-7). For instance, it can be seen that there is the presence of even masses that may be due to N containing compounds. This irregularity could be due to the greater fraction heterogeneity, i.e., composition diversity in O, N and alkyl C, compared to the mass spectra of the LMWF. This absence of a clear pattern as noted in (5-7) can also be the result of a structural diversity within the IMWF. Furthermore, the complexity of the mass spectrum could be due to the presence of singly but also doubly charged species or aggregates between neutral and singly charged species likely indicated by the high mass

defect of some masses along the series. As an example, mass defects of 0.8-0.9 are observed for masses in the range 700-800 Da. It is not possible up to now to determine straightforwardly the origin of this latter phenomenon in this IMWF. Further works would be needed to ascertain the IMWF characterization, particularly using exact masses determination and H/C and O/C correlations as in (7) or in (33).

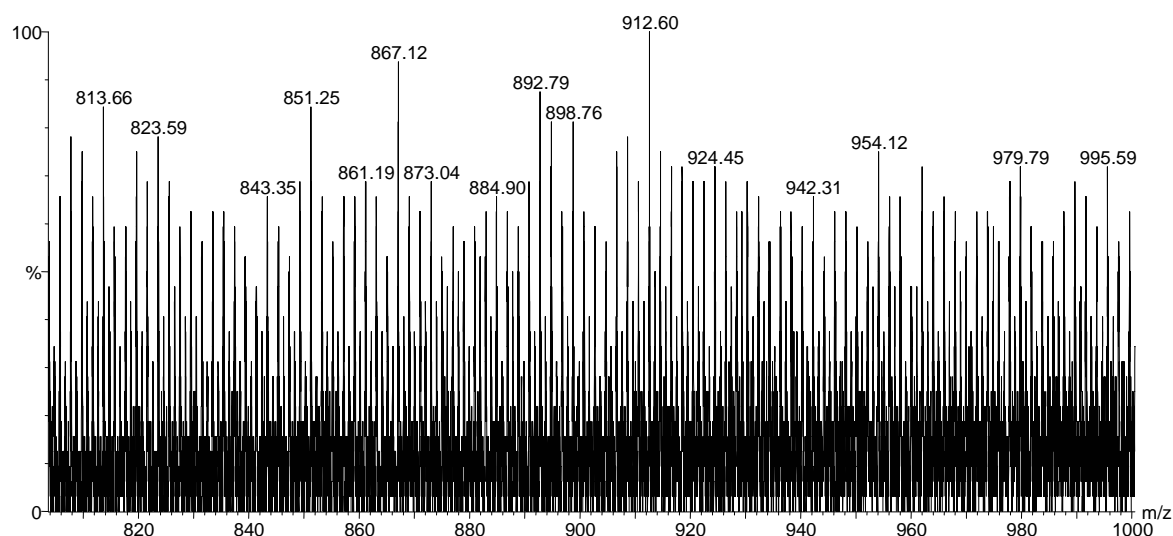


Figure 3: Influence of sorption of PAHA by 500 mg/L hematite on the ESI mass spectra of the supernatant at $\text{pH} \approx 7$, $[\text{PAHA}]^{\circ} = 33 \text{ mg/L}$, no background salt, IMWF detailed in the range 800-1000 Da.

Future developments should be the mandatory verification on environmental humic extracts to ascertain or discuss our conclusions. Further analysis of exact masses as well as H/C and O/C ratios after sorption should also be envisaged using higher resolution apparatus (7, 29, 33). Kinetic evolution of the phenomenon is also a crucial point to develop (15). Complementary information on sorbed species could also be obtained (54).

Crossing information from different techniques on the same extract(s) in order to have a global view of the fractionation phenomena, both in solution and on the surface should also be emphasized in view of identifying the reasons hidden behind the non additivity of binary systems when modeling ternary systems. If the fractionation evidenced here hides chemical fractionation, then one can also anticipate

even slight differences in complexation strength between the different factions that can explain this non additivity.

Acknowledgments. This work was partly financed through the Commission of the European Communities through the EC “HUPA project” (FIKW-CT-2001-00128), the MRTRA project of the Risk Control Domain of CEA (CEA/DEN/DDIN) and the CHSOL project of the Basis Research Domain of CEA (CEA/DEN/DSOE). Florence Casanova is acknowledged for her participation in the experimental work. The authors would like to acknowledge Dr. David A. Dzombak for his patience in editorial handling.

Supporting information gives complementary information about the experimental conditions used throughout the study, the values of absorbance at 203 and 253 nm and evolution of the ratio A_{253}/A_{203} , the absorbance spectra obtained for the initial PAHA sample and of supernatants from sorption experiments. Complementary ESI-QToF mass spectra are also given such as the verification of the influence of concentration on ESI mass spectra for a given sample, intermediate mass spectra of the supernatants that were not essential to the discussion and the evolution of number-averaged (\bar{I}_n) and weight-averaged (\bar{I}_w) mean molecular intensities.

References

- (1) Buffle, J. *Complexation reaction in aquatic system. An analytical approach*; Ellis-Horwood: Chichester, 1988.
- (2) Kersting, A. B.; Efurud, D. W.; Finnegan, D. L.; Rokop, D. J.; Smith, D. K.; Thompson, J. L., Migration of plutonium in groundwater at the Nevada Test Site. *Nature* **1999**, *397*, 56-58.
- (3) Wershaw, R. L., Model for Humus. *Environ. Sci. Technol.* **1993**, *27*, 814-816.
- (4) Piccolo, A.; Conte, P.; Cozzolino, A., Chromatographic and spectrophotometric properties of dissolved humic substances compared with macromolecular polymers. *Soil Sci.* **2001**, *166*, 174-185.
- (5) Plancque, G.; Amekraz, B.; Moulin, V.; Toulhoat, P.; Moulin, C., Molecular structure of fulvic acids by electrospray with quadrupole time-of-flight mass spectrometry. *Rapid Commun. Mass Spectrom.* **2001**, *15*, 827-835.
- (6) Moulin, V.; Reiller, P.; Amekraz, B.; Moulin, C., Direct characterization of iodine covalently bound to fulvic acids by electrospray mass spectrometry. *Rapid Commun. Mass Spectrom.* **2001**, *15*, 2488-2496.

- (7) Reemtsma, T.; These, A., Comparative investigation of low-molecular-weight fulvic acids of different origin by SEC-Q-TOF-MS: New insights into structure and formation. *Environ. Sci. Technol.* **2005**, *39*, 3507-3512.
- (8) Sutton, R.; Sposito, G., Molecular structure in soil humic substances: The new view. *Environ. Sci. Technol.* **2005**, *39*, 9009-9015.
- (9) Ochs, M.; Cosovic, B.; Stumm, W., Coordinative and hydrophobic interaction of humic substances with hydrophilic Al₂O₃ and hydrophobic mercury surfaces. *Geochim. Cosmochim. Acta* **1994**, *58*, 639-650.
- (10) Davis, J. A.; Gloor, R., Adsorption of dissolved organics in lake water by aluminum oxide. Effect of molecular weight. *Environ. Sci. Technol.* **1981**, *15*, 1223-1229.
- (11) Gu, B.; Schmitt, J.; Chem, Z.; Liang, L.; McCarthy, J. F., Adsorption and desorption of natural organic matter on iron oxide: mechanisms and models. *Environ. Sci. Technol.* **1994**, *28*, 38-46.
- (12) Meier, M.; Namjesnik-Dejanovic, K.; Maurice, P.; Chin, Y.-P.; Aiken, G. R., Fractionation of aquatic natural organic matter upon sorption to goethite and kaolinite. *Chem. Geol.* **1999**, *157*, 275-284.
- (13) Hur, J.; Schlautman, M. A., Molecular weight fractionation of humic substances by adsorption onto minerals. *J. Colloid Interface Sci.* **2003**, *264*, 313-321.
- (14) Hur, J.; Schlautman, M. A., Effects of pH and phosphate on the adsorptive fractionation of purified Aldrich humic acid on kaolinite and hematite. *J. Colloid Interface Sci.* **2004**, *277*, 264-270.
- (15) van de Weerd, H.; van Riemsdijk, W. H.; Leijnse, A., Modelling the dynamic adsorption/desorption of NOM mixture: Effects of physical and chemical heterogeneity. *Environ. Sci. Technol.* **1999**, *33*, 1675-1681.
- (16) Tombácz, E.; Libor, Z.; Illés, E.; Majzik, A.; Klumpp, E., The role of reactive surface sites and complexation by humic acids in the interaction of clay mineral and iron oxide particles. *Org. Geochem.* **2004**, *35*, 257-267.
- (17) Feng, X. J.; Simpson, A. J.; Simpson, M. J., Chemical and mineralogical controls on humic acid sorption to clay mineral surfaces. *Org. Geochem.* **2005**, *36*, 1553-1566.
- (18) Wang, K. J.; Xing, B. S., Structural and sorption characteristics of adsorbed humic acid on clay minerals. *J. Environ. Qual.* **2005**, *34*, 342-349.
- (19) Vermeer, A. W. P.; McCulloch, J. K.; van Riemsdijk, W. H.; Koopal, L. K., Metal ion adsorption to complexes of humic acid and metal oxides: deviation from the additivity rule. *Environ. Sci. Technol.* **1999**, *33*, 3892-3897.
- (20) Christl, I.; Kretzschmar, R., Interaction of copper and fulvic acid at the hematite-water interface. *Geochim. Cosmochim. Acta* **2001**, *65*, 3435-3442.
- (21) Davis, J. A., Complexation of trace metals by adsorbed natural organic matter. *Geochim. Cosmochim. Acta* **1984**, *48*, 679-691.
- (22) Takahashi, Y.; Minai, Y.; Ambe, S.; Makide, Y.; Ambe, F., Comparison of adsorption behavior of multiple inorganic ions on kaolinite and silica in the presence of humic acid using the multitracer technique - A comparison with dissolved aluminum. *Geochim. Cosmochim. Acta* **1999**, *63*, 815-836.
- (23) Reiller, P.; Casanova, F.; Moulin, V., Influence of addition order and contact time on thorium(IV) retention by hematite in the presence of humic acids. *Environ. Sci. Technol.* **2005**, *39*, 1641-1648.
- (24) McIntyre, C.; Batts, B. D.; Jardine, D. R., Electrospray mass spectrometry of groundwater organic acids. *J. Mass Spectrom.* **1997**, *32*, 328-330.
- (25) Persson, L.; Alsberg, T.; Kiss, G.; Odham, G., On-line size-exclusion chromatography/electrospray ionisation mass spectrometry of aquatic humic and fulvic acids. *Rapid Commun. Mass Spectrom.* **2000**, *14*, 286-292.
- (26) Leenheer, J. A.; Rostad, C. E.; Gates, P. M.; Furlong, E. T.; Ferrer, I., Molecular resolution and fragmentation of fulvic acid by electrospray ionization/multistage tandem mass spectrometry. *Anal. Chem.* **2001**, *73*, 1461-1471.

- (27) Fievre, A.; Solouki, T.; Marshall, A. G.; Cooper, W. T., High-resolution Fourier transform ion cyclotron resonance mass spectrometry of humic and fulvic acids by laser desorption/ionization and electrospray ionization. *Energy and Fuels* **1997**, *11*, 554-560.
- (28) Brown, T. L.; Rice, J. A., Effect of experimental parameters on the ESI FT-ICR mass spectrum of fulvic acid. *Anal. Chem.* **2000**, *72*, 384-390.
- (29) These, A.; Winkler, M.; Thomas, C.; Reemtsma, T., Determination of molecular formulas and structural regularities of low molecular weight fulvic acids by size-exclusion chromatography with electrospray ionization quadrupole time-of-flight mass spectrometry. *Rapid Commun. Mass Spectrom.* **2004**, *18*, 1777-1786.
- (30) Kujawinski, E. B.; Freitas, M. A.; Zang, X.; Hatcher, P. G.; Green-Church, K. B.; Jones, R. B., The application of electrospray ionization mass spectrometry (ESI MS) to the structural characterization of natural organic matter. *Org. Geochem.* **2002**, *33*, 171-180.
- (31) Stenson, A. C.; Landing, W. M.; Marshall, A. G.; Cooper, W. T., Ionization and fragmentation of humic substances in electrospray ionization Fourier transform-ion cyclotron resonance mass spectrometry. *Anal. Chem.* **2002**, *74*, 4397-4409.
- (32) Piccolo, A.; Spittler, M., Electrospray ionization mass spectrometry of terrestrial humic substances and their size fractions. *Anal Bioanal Chem* **2003**, *377*, 1047-1059.
- (33) Kujawinski, E. B.; Del Vecchio, R.; Blough, N. V.; Klein, G. C.; Marshall, A. G., Probing molecular-level transformation of dissolved organic matter: insight on photochemical degradation and protozoan modification of DOM from electrospray ionization Fourier transform ion cyclotron resonance mass spectrometry. *Mar. Chem.* **2004**, *92*, 23-37.
- (34) Stabenau, E. R.; Zika, R. G., Correlation of the absorption coefficient with a reduction in mean mass for dissolved organic matter in southwest Florida river plumes. *Mar. Chem.* **2004**, *89*, 55-67.
- (35) These, A.; Reemtsma, T., Structure-dependent reactivity of low molecular weight fulvic acid molecules during ozonation. *Environ. Sci. Technol.* **2005**, *39*, 8382-8387.
- (36) Caceci, M.; Moulin, V. Investigation of humic acid samples of different sources by photon correlation spectroscopy. In *Lecture Notes in Earth Sciences, Humic substances in the Aquatic and Terrestrial Environment*; Allard, B., Boren, H., Grimvall, A., Eds., 1991; Vol. 33, pp 97-104.
- (37) Kim, J. I.; Buckau, G.; Li, G. H.; Duschner, H.; Psarros, N., Characterization of humic and fulvic acids from Gorleben groundwater. *Fresenius J. Anal. Chem.* **1990**, *338*, 245-252.
- (38) Reiller, P.; Moulin, V.; Casanova, F.; Dautel, C., Retention behaviour of humic substances onto mineral surfaces and consequences upon thorium (IV) mobility: case of iron oxides. *Appl. Geochem.* **2002**, *17*, 1551-1562.
- (39) Vermeer, A. W. P., Interaction between humic acid and hematite and their effects upon metal speciation. Ph. D Thesis, Landbouwniversiteit Wageningen, Wageningen, 1996.
- (40) Monteil-Rivera, F.; Brouwer, E. B.; Masset, S.; Deslandes, Y.; Dumonceau, J., Combination of X-ray photoelectron and solid-state C-13 nuclear magnetic resonance spectroscopy in the structural characterisation of humic acids. *Anal. Chim. Acta* **2000**, *424*, 243-255.
- (41) Rice, J. A.; MacCarthy, J. F., Statistical evaluation of the elemental composition of humic substances. *Org. Geochem.* **1991**, *17*, 635-648.
- (42) Cromières, L.; Moulin, V.; Fourest, B.; Guillaumont, R.; Giffaut, E., Sorption of thorium onto hematite colloids. *Radiochim. Acta* **1998**, *82*, 249-256.
- (43) Cromières, L.; Moulin, V.; Fourest, B.; Giffaut, E., Physico-chemical characterization of the colloidal hematite/water interface: experimentation and modelling. *Colloid Surf. A-Physicochem. Eng. Asp.* **2002**, *202*, 101-115.
- (44) These, A.; Reemtsma, T., Limitations of electrospray ionization of fulvic and humic acids as visible from size exclusion chromatography with organic carbon and mass spectrometric detection. *Anal. Chem.* **2003**, *75*, 6275-6281.

- (45) Gu, B.; Mehlhorn, T. L.; Liang, L.; McCarthy, J. F., Competitive adsorption, displacement, and transport of organic matter on iron oxide: I. Competitive adsorption. *Geochim. Cosmochim. Acta* **1996**, *60*, 1943-1950.
- (46) Korshin, G. V.; Li, C.-W.; Benjamin, M. M., Monitoring the properties of natural organic matter through UV spectroscopy: a consistent theory. *Water Res.* **1997**, *31*, 1787-1795.
- (47) Reemtsma, T.; These, A., On-line coupling of size exclusion chromatography with electrospray ionization-tandem mass spectrometry for the analysis of aquatic fulvic and humic acids. *Anal. Chem.* **2003**, *75*, 1500-1507.
- (48) Shin, H. S.; Monsallier, J. M.; Choppin, G. R., Spectroscopic and chemical characterizations of molecular size fractionated humic acid. *Talanta* **1999**, *50*, 641-647.
- (49) Kaiser, K., Sorption of natural organic matter fractions to goethite (α -FeOOH): effect of chemical composition as revealed by liquid-state C-13 NMR and wet-chemical analysis. *Org. Geochem.* **2003**, *34*, 1569-1579.
- (50) Namjesnik-Dejanovic, K.; Maurice, P. A., Conformations and aggregate structures of sorbed natural organic matter on muscovite and hematite. *Geochim. Cosmochim. Acta* **2000**, *65*, 1047-1057.
- (51) Haddrell, A.; Agnes, G., Organic cation distributions in the residues of levitated droplets with net charge: Validity of the partition theory for droplets produced by an electrospray. *Anal. Chem.* **2004**, *76*, 53-61.
- (52) Kramer, R. W.; Kujawinski, E. B.; Hatcher, P. G., Identification of black carbon derived structures in a volcanic ash soil humic acid by Fourier transform ion cyclotron resonance mass spectrometry. *Environ. Sci. Technol.* **2004**, *38*, 3387-3395.
- (53) Gu, B.; Schmitt, J.; Chem, Z.; Liang, L.; McCarthy, J. F., Adsorption and desorption of different organic matter fraction on iron oxide. *Geochim. Cosmochim. Acta* **1995**, *59*, 219-229.
- (54) Claret, F.; Schafer, T.; Rabung, T.; Wolf, M.; Bauer, A.; Buckau, G., Differences in properties and Cm(III) complexation behavior of isolated humic and fulvic acid derived from Opalinus clay and Callovo-Oxfordian argillite. *Appl. Geochem.* **2005**, *20*, 1158-1168.

The sorption induced fractionation of Aldrich humic acid onto hematite is studied with ESI-QToF-MS, in order to identify missing fractions in the supernatant.